Fluid Phase Equilibria, 19 (1985) 175–200
Elsevier Science Publishers B.V., Amsterdam — Printed in The Netherlands

A NEW FORM OF THE EQUATION OF STATE FOR PURE SUBSTANCES AND ITS APPLICATION TO OXYGEN

R. SCHMIDT and W. WAGNER *

Institut für Thermo- und Fluiddynamik, Ruhr-Universität Bochum, Postfach 10 21 48, D 4630 Bochum 1 (W. Germany)

(Received March 16, 1984; accepted in final form August 31, 1984)

ABSTRACT

Schmidt, R. and Wagner, W., 1985. A new form of the equation of state for pure substances and its application to oxygen. *Fluid Phase Equilibria*, 19: 175–200.

A new wide range equation of state is presented and expressed analytically in the form of the free energy as a function of density and temperature. This fundamental equation contains, in addition to pure polynomial and "BWR"-terms, new exponential functions especially convenient for the critical region. To guarantee an effective structure, the combination of the terms of the equation was found by using an optimization method recently developed. As a result, the optimized function for the free energy is capable of representing the thermodynamic surface of oxygen in the range $54 \leq T \leq 300$ K, $0 < p \leq 818$ bar and $0 < \rho \leq 41$ mol dm^{-3} within the experimental uncertainty of the data available. With the exception of very few items of data, this statement is also valid for the whole coexistence curve and the critical region. Extrapolations of this new equation beyond the range of data yield physically meaningful results.

INTRODUCTION

The purpose of this study is to present an empirical equation of state for pure fluids which is able to describe the whole fluid region within the experimental uncertainty of the data. Oxygen was chosen as the test fluid for two reasons: (1) the existing thermodynamic tables for oxygen are based on equations of state which fail in some parts of the thermodynamic surface (critical region, phase boundary, velocity of sound of the saturated liquid); see for example Sytchev et al. (1981) and Younglove (1982); (2) the selected data provide an accurate description of the thermodynamic surface (thermal and caloric properties) including the coexistence curve and the critical region.

* Author to whom correspondence should be addressed.

0378-3812/85/$03.30

THE DEVELOPMENT OF WIDE RANGE EQUATIONS OF STATE

To illustrate the development of accurate equations of state representing the thermodynamic behaviour of pure fluids in the entire fluid range, some extended BWR-equations of state—originally not always established for oxygen—were refitted to the same selected data set of oxygen as used for fitting the new equation of state. The result appears in compressed form in Fig. 1. It describes the correlation between the number of adjustable coefficients N and the quality of the equation of state expressed by the weighted standard deviation q according to

$$q = \left(S^2/(M-N)\right)^{0.5} \tag{1}$$

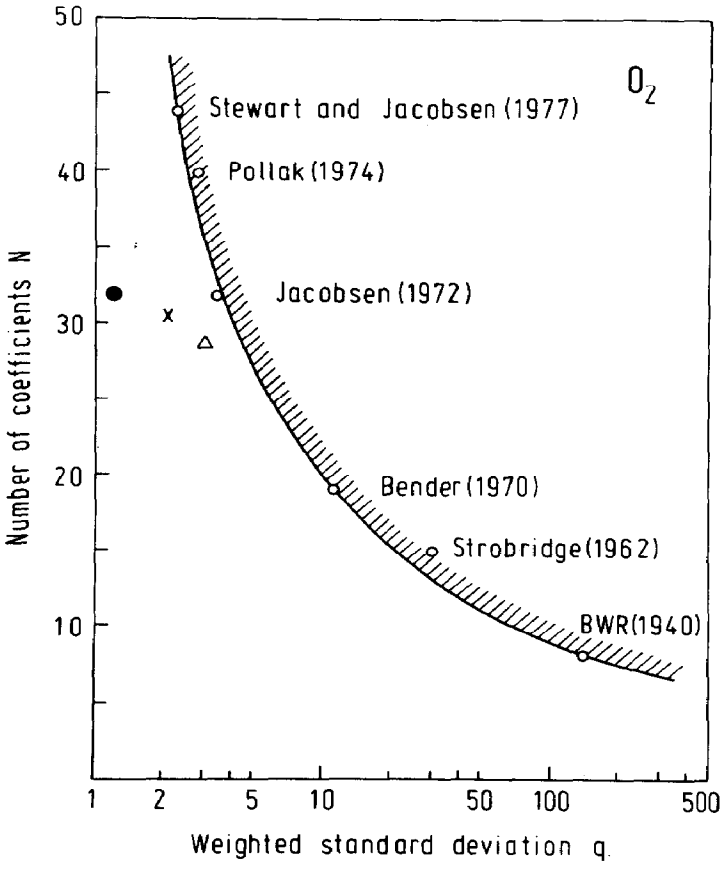

Fig. 1. Correlation between quality and number of adjusted coefficients of equations of state shown on the example of oxygen. BWR corresponds to the equation of state by Benedict et al. (1940). Δ, R.B. Stewart and R.T. Jacobsen (personal communication, 1980); ×, Ewers (1981); ●, this work.

where S^2 is the sum of weighted squares and M is the number of selected experimental data. The fitting of the equations referred to in Fig. 1 and the calculation of S^2 were performed in exactly the same way as used for the new equation of state. The line connects equations of state symbolized by the author's name, not optimized with respect to their structure. This means that the effect of the individual terms in these equations with respect to their number, their combination, and their form has not been analyzed with the help of an effective numerical procedure but that the terms have been determined subjectively by experience or by trial and error.

To overcome this situation Wagner (1974, 1977) developed a special version of a stepwise regression analysis for the optimization of functional expressions describing two-dimensional problems. This procedure has been applied successfully to vapour pressure equations (Baehr et al., 1976; Wagner et al., 1976; McGarry, 1983), orthobaric density equations (Pentermann and Wagner, 1978; Stewart et al., 1981) and for the ideal gas heat capacity (Wagner et al., 1982). The method was adapted by de Reuck and Armstrong (1979) and was applied to the equation of state problem. The triangle in Fig. 1 corresponds to an equation established by R.B. Stewart and R.T. Jacobsen (personal communication, 1980) with the adapted version of Wagner's regression analysis.

It is known that for the optimization of complex problems, random search strategies are superior to deterministic ones. Based on this knowledge, Ewers and Wagner (1981, 1982) developed a new procedure for optimizing the structure of equations of state, the so-called evolutionary optimization method (EOM). The cross in Fig. 1 represents the equation of state by Ewers (1981), which was established with the help of the EOM.

Figure 1 can be interpreted in the following way:

(1) the application of optimization techniques for the development of equations of state reduces considerably the number of coefficients N for a given quality q;

(2) even extended BWR equations optimized by the use of the EOM do not reach the limiting value $q = 1$. A value of $q = 1$ means that all data are represented within their experimental uncertainty. Hence, the "BWR"-functional form is not suitable for describing the whole thermodynamic surface accurately.

An analysis of these equations proves that they all fail to represent the thermodynamic properties in the critical and enlarged critical region, and some of the caloric data in the liquid. From these facts it was deduced that further improvements are only attainable by incorporating new functional forms in an equation of state.

DEVELOPMENT OF A NEW FUNCTIONAL FORM OF THE EQUATION OF STATE

The starting point for developing a new functional form of the equation of state was an analysis of the behaviour of wide range equations of state in the enlarged critical region. In Fig. 2 the status of these equations is shown with respect to thermal properties. In the pressure-density diagram, the solid line illustrates schematically a "true" isotherm for temperatures between the critical temperature T_c and $\sim 1.15\ T_c$ (the subscript c denotes the critical point). For densities near the critical density ρ_c, the known analytical equations of state are not able to describe the transition between the near horizontal course of the isotherm and the sections of marked change of curvature. For densities less than ρ_c, the calculated pressure is too low, and for densities higher than ρ_c it is too high (see the dashed line in Fig. 2). This statement also holds for equations which have been constrained to p_c, ρ_c, T_c, and to the conditions $(\partial p/\partial \rho)_c = (\partial^2 p/\partial \rho^2)_c = 0$. This shortcoming is often not observed because of the lack of accurate data in the enlarged critical region, but it exists nevertheless. To correct this failure a density function is needed which gives the contribution marked by the dotted area in Fig. 2.

For this purpose the expression $[\exp(-\delta^4) - \exp(-\delta^2)]$ has been chosen where $\delta = \rho/\rho_c$. As Fig. 3 shows, the difference of these exponential functions yields qualitatively such an area. To ensure a higher flexibility, this density correction function is multiplied by a polynomial with respect to density. In principle, this correction function can be incorporated in every wide range equation of state. Because of the widespread use of extended BWR-equations of state, this type of equation has been chosen as a "reference" equation.

The general structure of the equation of state is fixed as follows: (1) a

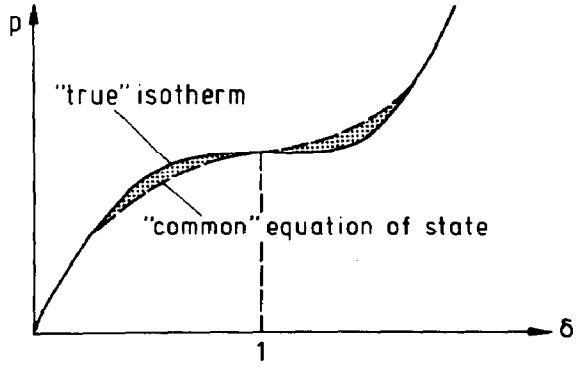

Fig. 2. The qualitative course of equations of state in the enlarged critical region with respect to thermal properties for temperatures between T_c and 1.15 T_c.

pure polynomial for δ and τ, Pol(δ, τ) with $\tau = T_c/T$; (2) a polynomial for δ and τ coupled with the exponential function $\exp(-\delta^2)$. Terms of the form Pol(δ, τ) $\exp(-\delta^2)$ are designated as BWR-terms; (3) the correction function $[\exp(-\delta^4) - \exp(-\delta^2)] \times$ Pol(δ, τ). Rearranging the three functional forms, the resulting dimensionless real part of the free energy Φ^r becomes:

$$\Phi^r = \frac{f^r}{RT} = \text{Pol}(\delta, \tau) + \text{Pol}(\delta, \tau)\exp(-\delta^2) + \text{Pol}(\delta, \tau)\exp(-\delta^4) \qquad (2)$$

where R is the universal gas constant, $\delta = \rho/\rho_c$, $\tau = T_c/T$ and $f^r = f - f^{id}$, where f^{id} is the free energy of the ideal gas at the same δ and τ. Terms of the form Pol(δ, τ) $\exp(-\delta^4)$ are denominated as E4-terms.

A further unsolved problem of wide range equations of state is the correct representation of the isochoric heat capacity c_v in the enlarged critical region, namely to follow the sharp increase of c_v when approaching T_c. Figure 4 illustrates this behaviour in a c_v, T diagram. For a critical or near critical isochore, the solid line shows schematically the "true" course of c_v, and the dashed line the calculated values from analytical equations of state. To correct this imperfection, according to

$$c_v = T(\partial^2 f/\partial T^2)_\rho \qquad (3)$$

a temperature function is needed whose second derivative strongly increases for temperatures $0.95\ T_c \lesssim T \lesssim 1.15\ T_c$.

Having chosen a polynomial to describe the temperature dependence of the real part of the free energy f^r, this requirement can be fulfilled by increasing the temperature exponents.

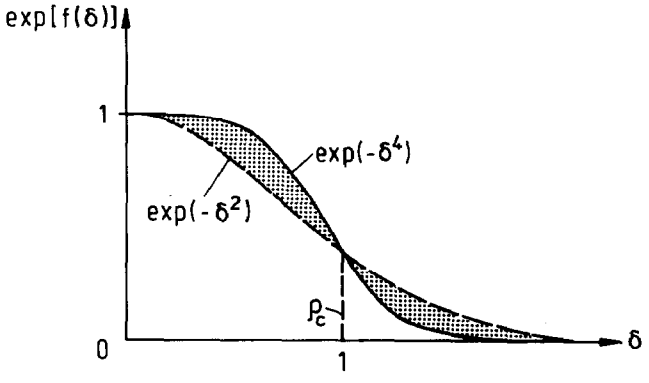

Fig. 3. The course of the functions $\exp(-\delta^2)$ and $\exp(-\delta^4)$ and their difference (dotted area).

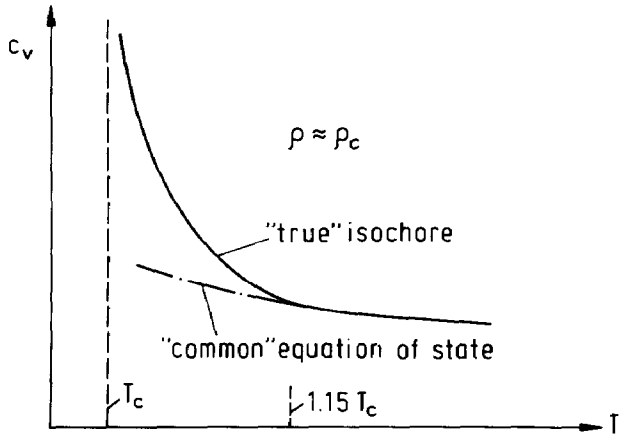

Fig. 4. The qualitative course of equations of state in the enlarged critical region with respect to caloric state variables shown on the example of c_v.

THE SELECTED DATA SET OF OXYGEN

In connection with an international joint equation of state project between the Institut für Thermo- und Fluiddynamik of the Ruhr-Universität Bochum (F.R.G.), the Center for Applied Thermodynamic Studies of the University of Idaho (U.S.A.) and the IUPAC-Thermodynamic Tables Project Centre, London (U.K.), a selected data set for the whole fluid region of oxygen has been established (R.B. Stewart and R.T. Jacobsen, personal communication, 1980; Schmidt, 1983). Table 1 gives information about the authors and about the range of the data used for fitting the equation of state.

TABLE 1

Selected data set of oxygen for establishing the equation of state (11)

Kind of data	Authors	Range		Number of data points
		T (K)	p (bar)	
p,ρ,T	Weber (1970a)	56 –300	6–362	1350
p,ρ,T	Weber (1977)	58 –300	35–818	324
p,ρ,T	Pentermann and Wagner (1978)	67 –300	0– 71	248
p,ρ,T	Ewers (1981)	56 –406	0–308	21
p_s,ρ',ρ'',T	Schmidt (1983)	54.4–154.6	0– 50.4	312
c_v,ρ,T	Goodwin and Weber (1969a)	56 –300	3–353	152
w,ρ,T	Van Itterbeek and Van Paemel (1938)	74 – 92	0– 1	41

The data set contains three different data forms: (1) pressure, density and temperature data of the homogeneous gas and liquid (p, ρ, T data), and of the coexistence liquid–gas curve (p_s, ρ', ρ'', T data); (2) isochoric heat capacities of the homogeneous phases (c_v, ρ, T data); and (3) velocities of sound of the low density region (w, ρ, T data). All data are experimental, with the following exceptions. (1) To extend the p, ρ, T data set to temperatures higher than 300 K, the data of Ewers (Ewers, 1981) were produced by the extrapolation of the unit compressibility line ($p/RT\rho = 1$); for details see Wagner et al. (1984). (2) From the reliable experimental data of the vapour pressure p_s, the saturated liquid density ρ' and the saturated vapour density ρ'', a p_s, ρ', ρ'', T data set had to be established for the following reason. To take into account the phase equilibrium condition (see eqn. (8)) for fitting the equation of state, the p_s, ρ', ρ'' data must be known at the same temperature. As these properties are measured independently as a function of temperature, experimental p_s, ρ', ρ'' data are not usually given at the same temperature. Therefore, the needed data set has been calculated for temperatures from 54.361 (triple point) to 150 K using the existing experimental data for ρ', a correlation equation for ρ' and ρ'' (Schmidt, 1983), a virial equation for the gas region (Wagner et al., 1984) and a vapour-pressure equation (Wagner et al., 1976). For temperatures from 150 to 154.571 K, there are ρ', ρ'', T data measured by Weber at the same temperatures. Again, the corresponding pressures, p_s, have been calculated using the vapour-pressure equation (Wagner et al., 1976). (3) The velocity of sound data was measured originally as a function of pressure and temperature. The use of such a w, p, T data set for fitting the equation of state would cause the fitting to be implicitly nonlinear. To avoid this complex fitting problem, the corresponding densities of the velocity of sound data were calculated for the experimental p, T values from a virial equation for oxygen established by Wagner et al. (1984).

In addition to these data, the selected data set also contains the following data forms: experimental p_s, ρ' and ρ'' values (for references see Fig. 6); isochoric heat capacities of the two-phase region (Goodwin and Weber, 1969b); velocities of sound of the homogeneous region (Van Itterbeek and Zink, 1958; Straty and Younglove, 1973) and of the saturated liquid line (Van Dael et al., 1966; Straty and Younglove, 1973). These data were not used for fitting the equation of state but for comparison only.

THE NEW EQUATION OF STATE

According to the report in the former paragraphs, the establishment of the equation of state was split into two steps: (1) formulation of a general expression for the equation of state which functions as a "bank of terms";

and (2) determining the most effective combination of a given number of terms out of the "bank of terms" using an optimization procedure.

In the first step, eqn. (2) was made accessible to the optimization method using the following expression for the general functional form of the real part of the free energy:

$$\Phi^{r,gen} = \frac{f^{r,gen}}{RT} = \sum_{i=1}^{I1} \sum_{j=1}^{J1} n_{i,j} \delta^{\alpha_i} \tau^{\beta_j} + e^{-\delta^2} \sum_{i=1}^{I2} \sum_{j=1}^{J2} n_{i,j} \delta^{\gamma_i} \tau^{\epsilon_j} + e^{-\delta^4} \sum_{i=1}^{I3} \sum_{j=1}^{J3} n_{i,j} \delta^{\zeta_i} \tau^{\eta_j} \tag{4}$$

with

$$\begin{aligned}
\alpha_i &= 1 + (i-1) && i = 1,2,\ldots, 9 \\
\beta_j &= -0.5 + (j-1) \times 0.5 && j = 1,2,\ldots,14 \\
\gamma_i &= 0 + (i-1) && i = 1,2,\ldots,11 \\
\epsilon_j &= 2 + (j-1) \times 0.5 && j = 1,2,\ldots,14 \\
\zeta_i &= 2 + (i-1) && i = 1,2,3,4 \\
\eta_j &= 10 + (j-1) && j = 1,2,\ldots,14
\end{aligned}$$

The ranges of the exponents α to η were chosen by experience.

In the second step, out of the bank of 336 terms defined by eqn. (4), the most effective combination of terms had to be found by the evolutionary optimization method (EOM) (Ewers and Wagner, 1982). Before starting the EOM, the total number of terms of the equation and the distribution of the terms to the three functional forms has to be fixed. Precalculations indicated that at least 32 coefficients in the combination—13 polynomial, 11 BWR and 8 E4 terms—are needed to fulfil the accuracy requirements, especially in the critical region. On this basis, using eqn. (4), the EOM creates populations of equations of state consisting of 32 terms, with each generation producing progressively improved quality. The quality criterion is the value of the sum of weighted squares (see eqn. (10)) obtained after fitting each of the equations to data using the maximum likelihood method.

As the EOM consumes a lot of computer time, the optimization is practically restricted to those data forms whose fitting leads to a system of linear equations to be solved with regard to the coefficients n_i. Consequently, the optimization was carried out by fitting to p, ρ, T data, to the phase equilibrium condition and to c_v data. According to the maximum likelihood method, using the relationship between the free energy and the different thermodynamic properties (see Appendix), and with the abbrevia-

tions of the partial derivatives

$$\Phi_\delta = (\partial\Phi/\partial\delta)_\tau \quad \Phi_{\delta\delta} = (\partial^2\Phi/\partial\delta^2)_\tau \quad \Phi_\tau = (\partial\Phi/\partial\tau)_\delta \quad \Phi_{\tau\tau} = (\partial^2\Phi/\partial\tau^2)_\delta$$
$$\Phi_{\delta\tau} = (\partial^2\Phi/\partial\delta\partial\tau) \tag{5}$$

the following three sums of weighted squares have to be minimized simultaneously.

(1) For all $M1$ p, ρ, T, $M2$ p_s, ρ', T and $M2$ p_s, ρ'', T data

$$S_1^2 = \sum_{m=1}^{M1+2M2} \left[\frac{p_m - \rho_m RT_m}{\rho_m^2 RT_m} - \frac{1}{\rho_c}\Phi_\delta^r(\delta_m, \tau_m) \right]^2 / \sigma_{1,m}^2 \tag{6}$$

(2) For all $M2$ p_s, ρ', ρ'', T data of the coexistence liquid–gas curve

$$S_2^2 = \sum_{m=1}^{M2} \left[\frac{p_{s,m}}{RT_m}\left(\frac{1}{\rho_m''} - \frac{1}{\rho_m'}\right) - \ln\left(\frac{\rho_m'}{\rho_m''}\right) - [\Phi^r(\delta_m', \tau_m) - \Phi^r(\delta_m'', \tau_m)] \right]^2 / \sigma_{2,m}^2 \tag{7}$$

Equation (7) corresponds to the fulfilling of the phase equilibrium condition with respect to the free energy

$$T' = T'' = T, \quad p' = p'' = p_s, \quad f' + p_s/\rho' = f'' + p_s/\rho'' \tag{8}$$

proposed by Bender (1970) and Wagner (1970, 1972) to be taken into account when fitting an equation of state to data of the whole fluid region.

(3) For all $M3$ c_v, ρ, T data

$$S_3^2 = \sum_{m=1}^{M3} \left[\frac{c_{v,m} - c_v^{id}(T_m)}{R} + \tau_m^2 \Phi_{\tau\tau}^r(\delta_m, \tau_m) \right]^2 / \sigma_{3,m}^2 \tag{9}$$

c_v^{id} denotes the isochoric heat capacity in the ideal gas state.

The variances $\sigma_{1,m}^2$, $\sigma_{2,m}^2$ and $\sigma_{3,m}^2$ were calculated with the help of the Gaussian error propagation formula with regard to the experimental uncertainty of pressure, density, temperature and heat capacity, respectively (for details see, Schmidt, 1983). The total sum of the weighted squares is then given by

$$S^2 = S_1^2 + S_2^2 + S_3^2 \tag{10}$$

As a result of having used the optimization procedure EOM, the final equation of state for oxygen has the form:

$$\Phi^r = \frac{f^r}{RT} = \sum_{i=1}^{13} n_i \delta^{r_i} \tau^{s_i} + e^{-\delta^2} \sum_{i=14}^{24} n_i \delta^{r_i} \tau^{s_i} + e^{-\delta^4} \sum_{i=25}^{32} n_i \delta^{r_i} \tau^{s_i} \tag{11}$$

with

i	r_i	s_i	i	r_i	s_i	i	r_i	s_i
1	1	0	14	1	5	25	2	22
2	1	1.5	15	1	6	26	3	11
3	1	2.5	16	2	3.5	27	3	18
4	2	−0.5	17	2	5.5	28	4	11
5	2	1.5	18	3	3	29	4	23
6	2	2	19	3	7	30	5	17
7	3	0	20	5	6	31	5	18
8	3	1	21	6	8.5	32	5	23
9	3	2.5	22	7	4			
10	6	0	23	8	6.5			
11	7	2	24	10	5.5			
12	7	5						
13	8	2						

At this step, the numerical values of the coefficients n_i are based on fitting eqn. (11) to p, ρ, T data, to the phase equilibrium condition and to c_v data only. However, to take into account the velocity of sound data also, the final determination of the coefficients n_i of eqn. (11) was performed by a nonlinear fitting, including the w data. The corresponding sum of weighted squares for all $M4$ w, ρ, T data is

$$S_4^2 = \sum_{m=1}^{M4} \left[\frac{w_m^2}{RT_m/M} - 1 - 2\delta_m \Phi_\delta^r - \delta_m^2 \Phi_{\delta\delta}^r + \frac{(1 + \delta_m \Phi_\delta^r - \delta_m \tau_m \Phi_{\delta\tau}^r)^2}{\tau_m^2 (\Phi_{\tau\tau}^{id} + \Phi_{\tau\tau}^r)} \right]^2 / \sigma_{4,m}^2 \tag{12}$$

where $\sigma_{4,m}^2$ was calculated from the total experimental uncertainties of the velocity of sound. Hence, the total sum of weighted squares according to

$$S^2 = S_1^2 + S_2^2 + S_3^2 + S_4^2 \tag{13}$$

had to be minimized, where S_1^2 to S_4^2 are related to eqns. (6), (7), (9) and (12), respectively.

To solve this nonlinear minimization problem, the modified Marquard method presented by Fletcher (1971) was used, as suggested by Ahrendts and Baehr (1979). The so-determined numerical values of the coefficients n_i of the new equation of state (11) are given in Table 2, together with the reducing parameters ρ_c and T_c, and the gas constant R.

To get the complete equation for f/RT, the dimensionless free energy of the ideal gas Φ^{id} has to be added to Φ^r according to

$$f/RT = \Phi_{eqn(15)}^{id} + \Phi_{eqn(11)}^r \tag{14}$$

The equation for Φ^{id} is obtained from an expression of the ideal gas heat

TABLE 2

Coefficients n_i of the equation of state (11)

i	n_i	i	n_i
1	0.3983768749	20	$0.1327699290\times10^{-1}$
2	$-0.1846157454\times10^{1}$	21	$-0.3254111865\times10^{-3}$
3	0.4183473197	22	$-0.8313582932\times10^{-2}$
4	$0.2370620711\times10^{-1}$	23	$0.2124570559\times10^{-2}$
5	$0.9771730573\times10^{-1}$	24	$-0.8325206232\times10^{-3}$
6	$0.3017891294\times10^{-1}$	25	$-0.2626173276\times10^{-4}$
7	$0.2273353212\times10^{-1}$	26	$0.2599581482\times10^{-2}$
8	$0.1357254086\times10^{-1}$	27	$0.9984649663\times10^{-2}$
9	$-0.4052698943\times10^{-1}$	28	$0.2199923153\times10^{-2}$
10	$0.5454628515\times10^{-3}$	29	$-0.2591350486\times10^{-1}$
11	$0.5113182277\times10^{-3}$	30	-0.1259630848
12	$0.2953466883\times10^{-6}$	31	0.1478355637
13	$-0.8687645072\times10^{-4}$	32	$-0.1011251078\times10^{-1}$
14	-0.2127082589		
15	$0.8735941958\times10^{-1}$		
16	0.1275509190	$R=$	8.31434 J mol^{-1} K^{-1}
17	$-0.9067701064\times10^{-1}$	$T_c=$	154.581 K
18	$-0.3540084206\times10^{-1}$	$\rho_c=$	13.63 mol dm^{-3}
19	$-0.3623278059\times10^{-1}$		

capacity of molecular oxygen developed by Wagner et al. (1982)

$$\Phi^{id}(\delta,\tau)=\frac{f^{id}(\delta,\tau)}{RT}=k_1\tau^{1.5}+k_2\tau^{-2}+k_3\ln\tau+k_4\tau+k_5\ln(e^{k_7\tau}-1)$$
$$+k_6\ln\left(1+\tfrac{2}{3}e^{-k_8\tau}\right)+k_9+\frac{h^{id}(\tau_0)}{RT}-\frac{s^{id}(\delta_0,\tau_0)}{R}+\ln\left(\frac{\delta}{\delta_0}\right) \quad (15)$$

where $\tau_0=T_c/T_0$, $\delta_0=p_0/(RT_0\rho_c)$, $T_0=298.15$ K and $p_0=1.01325$ bar. The values for $h^{id}(\tau_0)$ and $s^{id}(\delta_0,\tau_0)$ can be chosen arbitrarily; we have taken them to be zero.

With the coefficients k_i given in Table 3, eqn. (15) is valid for temperatures from 30 to 3000 K. (In this reference in eqn. (3) the square bracket should be after $1/(T/\mathrm{K})$; the last part of eqn. (4) should be $-\ln(p/p_0)$.) With eqn. (14) all thermodynamic properties of oxygen can be calculated. The appendix contains the relationships between Φ and the most common thermodynamic properties, and the needed derivatives of Φ, in an explicit form. In the forthcoming IUPAC book on oxygen (Angus et al., in prep.) thermodynamic tables based on eqn. (14) will be published.

TABLE 3

The coefficients k_i of eqn. (15)

i	k_i	i	k_i
1	-0.740775×10^{-3}	7	0.145066×10^{2}
2	-0.664930×10^{-4}	8	0.749148×10^{2}
3	0.250042×10^{1}	9	0.414817×10^{1}
4	-0.214487×10^{2}		
5	0.101258×10^{1}	$R=$	8.31434 J mol^{-1} K^{-1}
6	-0.944365×10^{0}	$T_c=$	154.581 K

COMPARISON OF THE NEW EQUATION OF STATE WITH DATA

The global quality of the new equation of state (14) is shown by a full circle in Fig. 1. With this equation, the optimum value $q = 1$ has nearly been reached. With regard to the quantity $(q - 1)$ the improvement, compared with optimized extended BWR equations with comparable length, is more than 100%. This improvement is exclusively caused by the new E4-terms.

To illustrate the quality of the new equation in more detail, some comparisons of eqn. (11) or (14) to various data forms are given.

p, ρ, T data

Figure 5 shows the percentage density deviation on three selected isotherms. For the subcritical 140 K isotherm the dashed lines separate the two-phase region; the solid symbols show the saturated vapour and saturated liquid density, respectively. The 3σ lines, which limit the range of the total experimental uncertainty with respect to density, are plotted as deviations from the corresponding equation of state values. Thus, it can be seen that all p, ρ, T data on the three isotherms are represented within the experimental error. This behaviour can be found for all p, ρ, T data (see Schmidt, 1983). The existing equations of state with a similar number of parameters show, especially for isotherms slightly above T_c, deviations which are more than six times larger.

Thermal properties on the coexistence curve

Figure 6 shows the deviations between experimental and calculated values with respect to vapour pressure, saturated liquid density and saturated vapour density. For a given temperature the equation of state yields these properties by applying only the phase equilibrium condition (8), without using auxiliary equations. A comparison of the deviations with the corre-

sponding variances shows that for the entire temperature range all three properties are represented within the experimental uncertainty. For the temperature range $(T_c - T) \leq 0.4$ K the deviation is just outside the experimental uncertainty; details will be given later. Nevertheless, up to now, no equation of state for oxygen is known which achieves this quality. The excellent agreement of the equation of state with the experimental data underlines that the "artificial" p_s, ρ', ρ'', T data set used for fitting the equation was reasonable.

Caloric data

The representation of caloric data makes high demands on equations of state since various derivatives of the fundamental equation are needed. For example, the calculation of c_v requires correct second temperature derivatives of the free energy (see eqn. (3)). The capability of the new equation of state to represent both thermal and caloric data is shown by the example of the velocity of sound w' of the saturated liquid. Although these data were

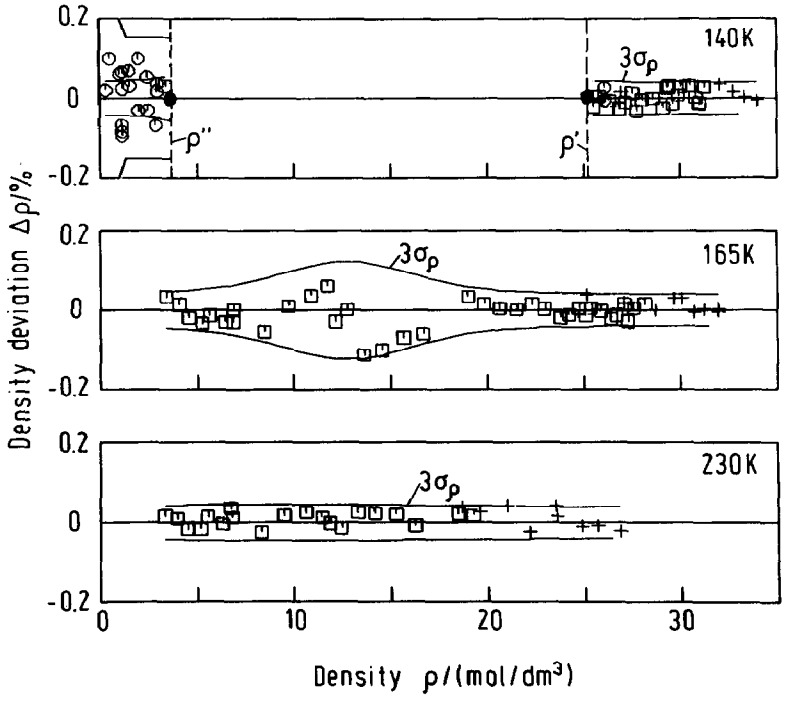

Fig. 5. Percentage density deviations $\Delta\rho = (\rho_m - \rho_{eqn(14)})/\rho_m$ of the selected p, ρ, T data from the values calculated using eqn. (14) on three characteristic isotherms. ○, Pentermann and Wagner (1978); □, Weber (1970a); +, Weber (1977).

not included in the simultaneous fitting, their representation is excellent.

Figure 7 shows the relative deviations of the selected w' data as a function of temperature. For a large temperature range, the deviations $\Delta w'$ remain smaller than 0.2%. For near critical temperatures, the w' data of Straty and Younglove (1973) and of Van Dael et al. (1966) have different tendencies relative to eqn. (14). The calculated w' values lie in the temperature range between the two data forms and, therefore, provide a good estimation of the "true" value of w'.

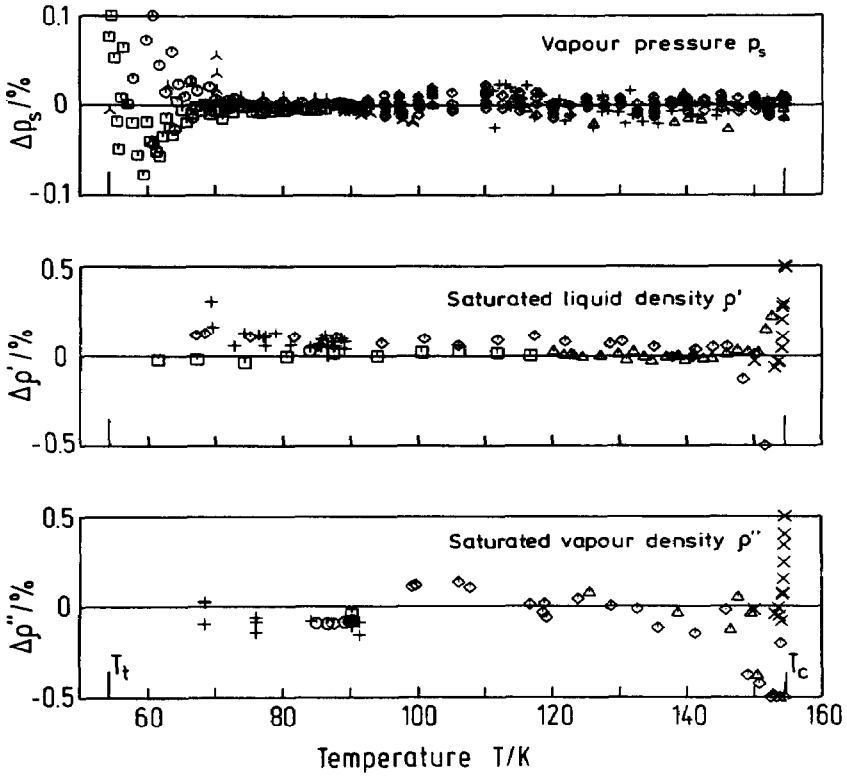

Fig. 6. Percentage deviations $\Delta y = (y_m - y_{eqn(14)})/y_m$ of the experimental saturation data from the corresponding equation of state values with $y = p_s, \rho'$ or ρ'', respectively. For the density data being on the boundary see Table 4. *Vapour pressure*: □, ○, Ancsin (1974, personal communication, 1976); +, Hoge (1950); ×, Mochizuki et al. (1969, personal communication, 1976); λ, Tiggelman (1973); ◇, Wagner et al. (1976); △ Weber (1970a). *Saturated liquid density*: △, Weber (1970a); ×, Weber (1970b); ○, Pool et al. (1962); +, Baly and Donnan (1902); ◇, Pentermann and Wagner (1978); □, calculated by Pentermann (1977) from Weber (1970a). *Saturated vapour density*: +, calculated from Furukawa and McCoskey (1953); ○, calculated from Suyama and Oishi (1976); □, calculated from Clusius and Konnertz (1949); Y, calculated from Frank and Clusius (1939); △, Weber (1970a); ×, Weber (1970b); ◇, Pentermann and Wagner (1978).

For temperatures near the triple point temperature T_t, both data sets deviate systematically from the calculated w' values by increasing deviations up to 2% for temperatures near T_t. This deviation is probably caused by small inconsistencies in the selected data set of oxygen. It should be mentioned, however, that even deviations of 2% are commonly regarded as good (Angus et al., 1978), and often equations used for compiling tables represent w' near T_t with errors of ~ 20% (Angus et al., 1979; Sytchev et al., 1981). Not only w' data, but also other measured caloric data, are represented very well. For the c_v data of the homogeneous region (Goodwin and Weber, 1969a) and in the two-phase region (Goodwin and Weber, 1969b) the deviations between the measured and calculated values are smaller than the reported experimental uncertainty of ~ 1%. The agreement between measured and calculated velocities of sound is good. On a few isotherms there are small systematic deviations which are probably caused by small inconsistencies between those w data and the other data forms. The known wide range equations of state for oxygen exhibit a similar behaviour (Jacobsen, 1972).

The critical and enlarged critical region

Up to now, no analytical equation of state is known which represents, in addition to the conventional surface, both thermal and caloric data in the critical and enlarged critical region. In Figure 8, the behaviour of the new equation of state for the thermal properties in the critical region is shown. The representation of the p, ρ, T data in the critical region is a specially severe criterion of judging an equation of state. The p, ρ diagram describes the medium density region around the critical point for temperatures about ± 1.5 K around T_c. The coexistence curve and the isotherms, plotted by solid lines, were calculated from the equation of state (14). It is obvious that the

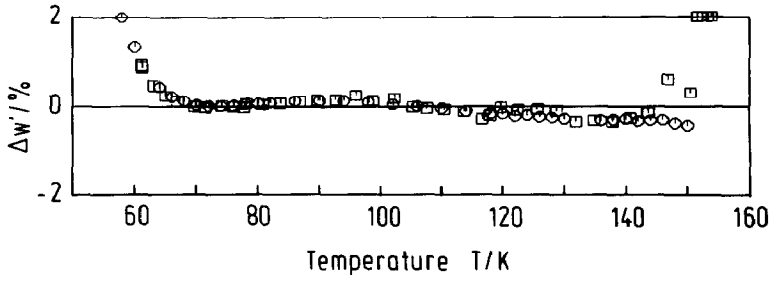

Fig. 7. Percentage velocity of sound deviations of the saturated liquid $\Delta w' = (w'_m - w'_{eqn(14)})/w'_m$ of the selected w' data from the values calculated using eqn. (14). ○, Straty and Younglove (1973); □, Van Dael et al. (1966).

experimental orthobaric densities and p, ρ, T data on the 156 K isotherm are represented accurately. Table 4 shows the numerical values of the deviations between the experimental and calculated orthobaric densities, together with the experimental uncertainties. As for all other data, the values determined experimentally for the critical point are subject to uncertainties. For that reason it was intentionally renounced to constrain the equation of state to the internationally accepted critical point value given by Weber (1970b). Table 5 gives values for the critical point calculated from the new equation of state, and Weber's values for comparison. The difference between the calculated critical point parameters and Weber's values resulting from dielectric constant measurements is approximately the order of magnitude of the uncertainties given by Weber (1970b) with respect to all three parameters.

The representation of caloric data in this area is visualized on the basis of

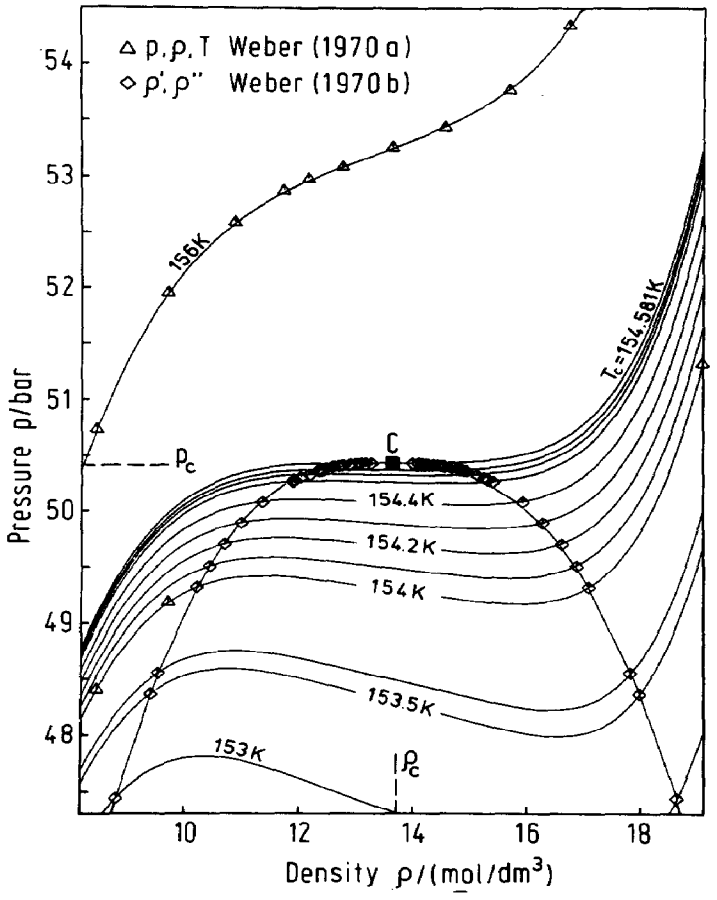

Fig. 8. The representation of thermal properties in the enlarged critical region using eqn. (14).

TABLE 4

Comparison of the experimental orthobaric densities (Weber, 1970a, 1970b) with those calculated using eqn. (14) with the experimental uncertainties σ

$\Delta\rho = (\rho_{exp} - \rho_{calc})/\rho_{exp}$

T(K)	ρ'_{exp} (mol dm^{-3})	ρ'_{calc} (mol dm^{-3})	$\Delta\rho'$ (%)	$\sigma_{\rho'}$ (%)	ρ''_{exp} (mol dm^{-3})	ρ''_{calc} (mol dm^{-3})	$\Delta\rho''$ (%)	$\sigma_{\rho''}$(%)
150.000	21.1093	21.1096	−0.027	0.084	6.71588	6.71701	−0.017	0.105
150.540	20.7640	20.7599	0.020	0.085	6.98934	7.00186	−0.179	0.107
153.003	18.6351	18.6468	−0.063	0.098	8.81596	8.81960	−0.041	0.134
153.504	17.9819	17.9879	−0.033	0.109	9.40973	9.41053	−0.008	0.153
153.604	17.8288	17.8340	−0.029	0.113	9.54411	9.54915	−0.053	0.158
154.004	17.0944	17.0867	0.045	0.140	10.2129	10.2210	−0.079	0.197
154.104	16.8819	16.8471	0.206	0.153	10.4410	10.4342	0.065	0.215
154.105	16.8631	16.8446	0.110	0.153	10.4441	10.4365	0.073	0.216
154.204	16.6163	16.5704	0.276	0.173	10.6941	10.6782	0.149	0.241
154.304	16.2850	16.2373	0.293	0.206	10.9942	10.9671	0.247	0.282
154.401	15.9256	15.8218	0.652	0.282	11.3567	11.3178	0.343	0.367
154.495	15.4006	15.2359	1.070	0.439	11.8848	11.7908	0.791	0.549
154.505	15.3037	15.1530	0.985	0.474	11.9036	11.8557	0.402	0.589
154.515	15.2412	15.0637	1.165	0.519	12.0254	11.9252	0.833	0.639
154.528	15.1256	14.9361	1.253	0.598	12.1817	12.0237	1.297	0.727
154.545	14.9318	14.7434	1.262	0.770	12.3380	12.1714	1.351	0.915
154.549	14.8693	14.6926	1.188	0.833	12.4161	12.2101	1.659	0.983
154.551	14.8193	14.6663	1.032	0.869	12.4505	12.2302	1.769	1.022
154.565	14.5506	14.4607	0.618	1.322	12.5911	12.3876	1.616	1.506
154.571	14.4287	14.3578	0.491	1.812	12.8755	12.4670	3.173	2.022
154.571	14.4568	14.3578	0.685	1.812	12.7630	12.4670	2.319	2.022

The experimental uncertainty σ_ρ has been calculated using the error propagation formula with $\Delta T = 0.009$ K and $\sigma_\rho = 8\times10^{-4}\ \rho$ for $T < 154.401$ K and $\sigma_\rho = 1.2\times10^{-3}\ \rho$ for $T \geq 154.401$ K.

TABLE 5

Parameter values for the critical point

	Experimentally determined by Weber (1970b)	Calculated from eqn. (14)
p_c (bar)	50.43	50.46
ρ_c (mol dm^{-3})	13.63	13.34
T_c (K)	154.581	154.599

a $c_v^r/R,T$ diagram in Fig. 9 where the real part of the isochoric heat capacity c_v^r is defined by $c_v^r = -R\tau^2\Phi_{\tau\tau}^r$. The circles in Fig. 9 show the real part of the c_v data of Goodwin and Weber (1969a) for a near critical isochore. The line represents the values calculated from eqn. (11). The vertical bars at some data points indicate the total experimental uncertainty. It can be seen that

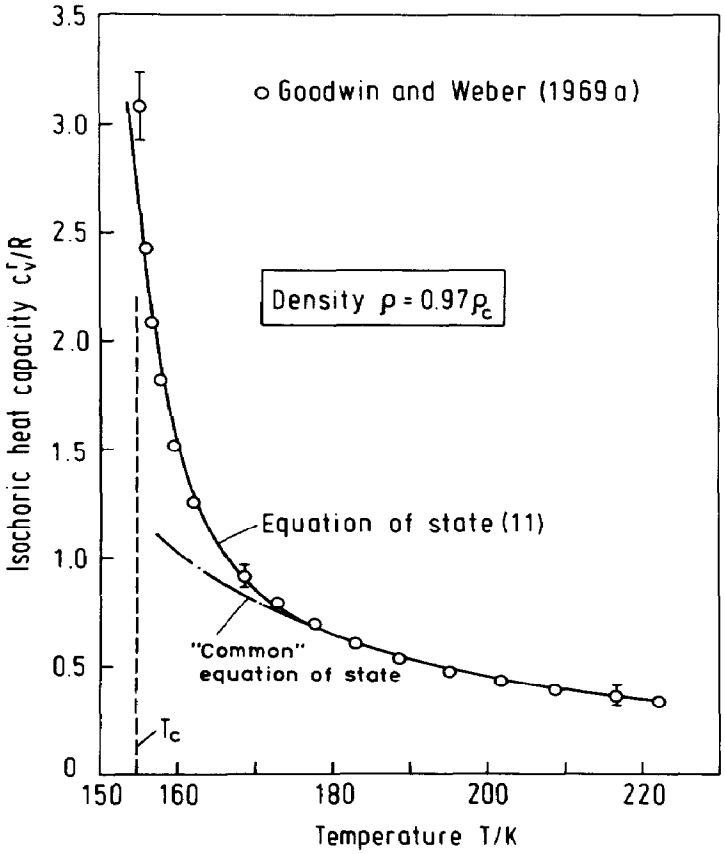

Fig. 9. The representation of c_v^r/R on a near critical isochore using eqn. (11).

the calculated values actually follow the sharp increase of c_v^r approaching T_c. The difference between the measured and calculated values is in all cases smaller than the experimental uncertainty, with the exception of the data point nearest to T_c. Extended BWR-equations with comparable length provide the dashed-dotted line.

Although the equation of state represents the experimental data of the critical region in the vast majority of cases within experimental uncertainty, the equation does not yield the critical exponents derived from the experiment. Furthermore, the equation does not yield an infinite, but a very large value of c_v^r at the critical point.

Extrapolation

To finish the discussion of the new equation of state, its extrapolation capability is examined with the help of Fig. 10. The p, ρ diagram shows the 300 K isotherm, which is the highest temperature for which reliable p, ρ, T data exist. The line represents the course resulting from equation (14), and the hatched line bounds the region for which data on this isotherm exist. The extrapolated part of this line yields physically meaningful results. This statement is underlined by the fact that two semi-empirical equations give similar results. The circles correspond to values calculated using the Deiters equation (Deiters, 1981) and the squares to the so-called "base function" developed by Haar et al. (1980, personal communication, 1981). Both

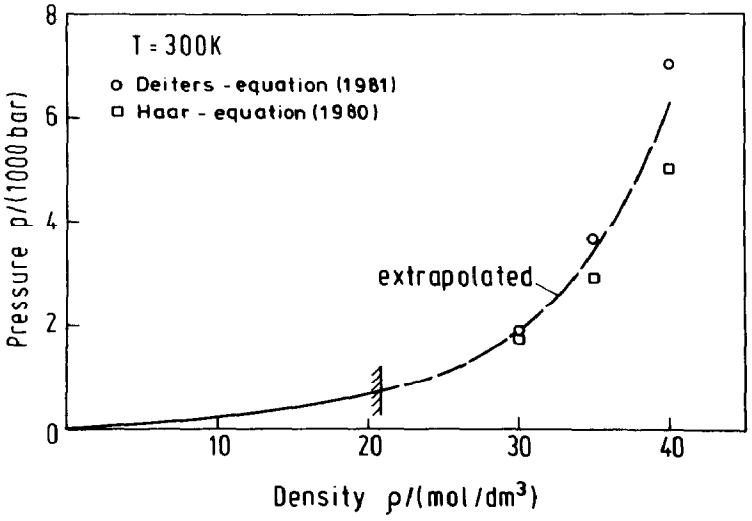

Fig. 10. Extrapolation test of eqn. (14) with respect to thermal properties shown by the example of the 300 K isotherm.

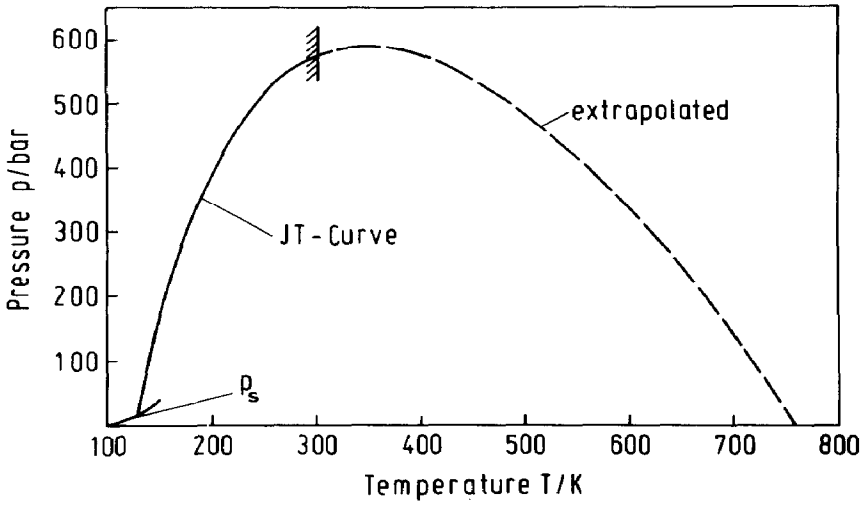

Fig. 11. The course of the Joule–Thomson (JT) curve calculated using eqn. (11).

equations use modified Carnahan–Starling equations (Carnahan and Starling, 1972) for the repulsive forces between molecules. An isochoric extrapolation also gives reasonable results (see Schmidt, 1983). Moreover, the equation yields a realistic course for extrapolated values of derived properties. This is shown in Fig. 11 for the Joule–Thomson (JT) curve, for which

$$\left(\frac{\partial T}{\partial p}\right)_h = \frac{1}{c_p}\left[\frac{T(\partial p/\partial T)_\rho}{\rho^2(\partial p/\partial \rho)_T} - \frac{1}{\rho}\right] \tag{16}$$

equals zero. In eqn. (16), c_p denotes the specific heat capacity at constant pressure. The line represents the calculated JT curve. The dotted part of this line lies in the region where no experimental data for oxygen exist. Again, the course of the JT curve is physically meaningful. Even the inversion temperature T_{inv}, determined by this extrapolation to be ~ 770 K, agrees very well with the expectation $T_{inv} \simeq 1.9\ T_B$ with the Boyle temperature $T_B \simeq 406$ K (Wagner et al., 1984).

CONCLUSION

Based on the shortcomings of the known wide range equations of state, especially in the critical region, a new general form of the fundamental equation for the free energy of pure substances has been developed. With this background, and with the help of an optimization procedure, an effective equation of state of oxygen in form of the free energy has been established.

The new oxygen equation of state represents nearly all experimental

thermal and caloric data, which are considered to be reliable, within the experimental uncertainty. This statement is not only valid for the homogeneous phases, but also for the coexistence vapour–liquid curve and for the critical region. This quality statement gains importance because the selected data set contains ~ 3000 p, ρ, T items of data of the homogeneous phases and coexistence curve, isochoric heat capacities, and velocities of sound. The whole data set covers a temperature range from the triple point temperature (54 K) to 400 K at pressures up to 818 bar, and densities up to three times the critical density. Furthermore, the equation allows meaningful extrapolations beyond the range of data.

ACKNOWLEDGEMENT

The authors thank Mrs. P. Leyens for her help with the development of the computer programs.

LIST OF SYMBOLS

c_p	molar isobaric heat capacity
c_v	molar isochoric heat capacity
f	molar free energy
g	molar free enthalpy
h	molar enthalpy
i, j, m	serial numbers
k	coefficient
M	number of selected experimental data; molecular mass ($M_{O_2} = 31.9988$ g mol^{-1})
n	coefficient
N	number of coefficients
p	pressure
q	standard deviation
r	exponent of density
R	universal gas constant ($= 8.31434$ J mol^{-1} K^{-1})
S^2	weighted sum of squares
s	molar entropy
t	exponent of temperature
T	thermodynamic temperature, IPTS 68
u	molar energy
v	molar volume
w	velocity of sound
$\alpha, \beta, \gamma, \epsilon, \zeta, \eta$	exponents
δ	reduced density ($= \rho/\rho_c$)

Δ	deviation
ρ	molar density
σ	standard deviation, experimental uncertainty
τ	reciprocal reduced temperature ($= T_c/T$)
Φ	dimensionless free energy ($= f/RT$)

Subscripts

B	Boyle point
c	at the critical point
inv	inversion point
i	serial number
j	serial number
m	measured value
s	at saturation
t	at the triple point
0	reference state

Superscripts

r	real part of
$'$	saturated liquid
$''$	saturated vapour
id	in the ideal gas state

APPENDIX

For some common state variables, the relation to the dimensionless free energy Φ is given:

Pressure p: $p = \rho RT(1 + \delta\Phi_\delta^r)$ (A1)

Internal energy: $\dfrac{u(\delta, \tau)}{RT} = \tau\left(\Phi_\tau^{id} + \Phi_\tau^r\right)$ (A2)

Enthalpy h: $\dfrac{h(\delta, \tau)}{RT} = 1 + \tau\left(\Phi_\tau^{id} + \Phi_\tau^r\right) + \delta\Phi_\delta^r$ (A3)

Entropy s: $\dfrac{s(\delta, \tau)}{R} = \tau\left(\Phi_\tau^{id} + \Phi_\tau^r\right) - \Phi^{id} - \Phi^r$ (A4)

Free enthalpy g: $\dfrac{g(\delta, \tau)}{RT} = 1 + \Phi^{id} + \Phi^r + \delta\Phi_\delta^r$ (A5)

Isochoric heat capacity c_v: $\dfrac{c_v(\delta, \tau)}{R} = -\tau^2\left(\Phi_{\tau\tau}^{id} + \Phi_{\tau\tau}^r\right)$ (A6)

Isobaric heat capacity c_p: $$\frac{c_p(\delta,\tau)}{R} = \frac{c_v(\delta,\tau)}{R} + \frac{\left(1+\delta\Phi^r_\delta - \delta\tau\Phi^r_{\delta\tau}\right)^2}{1+2\delta\Phi^r_\delta + \delta^2\Phi^r_{\delta\delta}} \tag{A7}$$

Velocity of sound w: $$\frac{w^2(\delta,\tau)}{RT/M} = 1 + 2\delta\Phi^r_\delta + \delta^2\Phi^r_{\delta\delta} - \frac{\left(1+\delta\Phi^r_\delta - \delta\tau\Phi^r_{\delta\tau}\right)^2}{\tau^2\left(\Phi^{id}_{\tau\tau} + \Phi^r_{\tau\tau}\right)} \tag{A8}$$

To ease the practical application of eqns. (A1)–(A8) in connection with eqn. (14), the needed derivatives of Φ^{id} and Φ^r are specified:

1st derivative of the dimensionless free energy Φ with respect to the reduced density δ:

$$\Phi^{id}_\delta = 1/\delta \tag{A9}$$

$$\Phi^r_\delta = \sum_i n_i r_i \delta^{(r_i-1)}\tau^{s_i} + \exp(-\delta^2)\sum_i n_i\left[r_i\delta^{(r_i-1)} - 2\delta^{(r_i+1)}\right]\tau^{s_i} + \exp(-\delta^4)\sum_i n_i\left[r_i\delta^{(r_i-1)} - 4\delta^{(r_i+3)}\right]\tau^{s_i} \tag{A10}$$

2nd derivative of the dimensionless free energy Φ with respect to the reduced density δ:

$$\Phi^{id}_{\delta\delta} = -1/\delta^2 \tag{A11}$$

$$\Phi^r_{\delta\delta} = \sum_i n_i r_i(r_i-1)\delta^{(r_i-2)}\tau^{s_i} + \exp(-\delta^2)\sum_i n_i\left[r_i(r_i-1)\delta^{(r_i-2)} - 2(2r_i+1)\delta^{r_i} + 4\delta^{(r_i+2)}\right]\tau^{s_i} + \exp(-\delta^4)\sum_i n_i\left[r_i(r_i-1)\delta^{(r_i-2)} - 4(2r_i+3)\delta^{(r_i+2)} + 16\delta^{(r_i+6)}\right]\tau^{s_i} \tag{A12}$$

1st derivative of the dimensionless free energy Φ with respect to the reciprocal reduced temperature τ:

$$\Phi^{id}_\tau = 1.5k_1\tau^{0.5} - 2k_2\tau^{-3} + k_3\tau^{-1} + k_4 + k_5\frac{k_7\exp(k_7\tau)}{\exp(k_7\tau)-1} - k_6\frac{\frac{2}{3}k_8\exp(-k_8\tau)}{1+\frac{2}{3}\exp(-k_8\tau)} \tag{A13}$$

$$\Phi^r_\tau = \sum_i n_i s_i \delta^{r_i}\tau^{(s_i-1)} + \exp(-\delta^2)\sum_i n_i s_i\delta^{r_i}\tau^{(s_i-1)} + \exp(-\delta^4)\sum_i n_i s_i\delta^{r_i}\tau^{(s_i-1)} \tag{A14}$$

2nd derivative of the dimensionless free energy Φ with respect to the

reciprocal reduced temperature τ:

$$\Phi_{\tau\tau}^{id} = 0.75k_1\tau^{-0.5} + 6k_2\tau^{-4} - k_3\tau^{-2} - k_5\frac{k_7^2\exp(k_7\tau)}{[\exp(k_7\tau)-1]^2} + k_6\frac{\frac{2}{3}k_8^2\exp(-k_8\tau)}{[\frac{2}{3}\exp(-k_8\tau)+1]^2} \quad \text{(A15)}$$

$$\Phi_{\tau\tau}^{r} = \sum_i n_i s_i(s_i-1)\delta^{r_i}\tau^{(s_i-2)} + \exp(-\delta^2)\sum_i n_i s_i(s_i-1)\delta^{r_i}\tau^{(s_i-2)} + \exp(-\delta^4)\sum_i n_i s_i(s_i-1)\delta^{r_i}\tau^{(s_i-2)} \quad \text{(A16)}$$

1st mixed derivative of the dimensionless free energy Φ with respect to the reduced density δ and the reciprocal reduced temperature τ:

$$\Phi_{\delta\tau}^{id} = 0 \quad \text{(A17)}$$

$$\Phi_{\delta\tau}^{r} = \sum_i n_i r_i s_i \delta^{(r_i-1)}\tau^{(s_i-1)} + \exp(-\delta^2)\sum_i n_i\left(r_i\delta^{(r_i-1)} - 2\delta^{(r_i+1)}\right)s_i\tau^{(s_i-1)} + \exp(-\delta^4)\sum_i n_i\left(r_i\delta^{(r_i-1)} - 4\delta^{(r_i+3)}\right)s_i\tau^{(s_i-1)} \quad \text{(A18)}$$

REFERENCES

Ahrendts, J. and Baehr, H.D., 1979. Die direkte Verwendung von Messwerten beliebiger thermodynamischer Zustandsgrössen zur Bestimmung kanonischer Zustandsgleichungen. Forsch. Ing.-Wes., 45: 1–36.

Angus, S., Armstrong, B. and de Reuck, K.M., 1978. International Thermodynamic Tables of the Fluid State—5, Methane. Pergamon Press, Oxford.

Angus, S., Armstrong, B., de Reuck, K.M., Stewart, R.B. and Jacobsen, R.T., 1979. International Thermodynamic Tables of the Fluid State—6, Nitrogen. Pergamon Press, Oxford.

Angus, S., de Reuck, K.M. Stewart, R.B. and Wagner, W., in prep. International Thermodynamic Tables of the Fluid State—9, Oxygen (to be published).

Ancsin, J., 1974. Vapour pressure scale of oxygen. Can. J. Phys., 52: 2305–2312.

Baehr, H.D., Garnjost, H. and Pollak, R., 1976. The vapour pressure of liquid ammonia—new measurements above 328 K and a rational vapour pressure equation. J. Chem. Thermodyn., 8: 113–119.

Baly, E.C.C. and Donnan, F.G., 1902. The variation with temperature of the surface energies of liquid oxygen, nitrogen, argon and carbon monoxide. J. Chem. Soc., 81: 907–923.

Bender, E., 1970. Equations of state exactly representing the phase behaviour of pure substances. In: Proc. Fifth Symp. on Thermophysical Properties, Am. Soc. Mech. Eng., 227–235.

Benedict, M., Webb, G.B. and Rubin, L.C., 1940. An empirical equation for thermodynamic properties of light hydrocarbons and their mixtures. I. Methane, ethane, propane and *n*-butane. J. Chem. Phys., 8: 334–345.

Carnahan, N.F. and Starling, K.E., 1972. Intermolecular repulsions and the equation of state for fluids. AIChE J., 18: 1184–1189.

Clusius, K. and Konnertz, F., 1949. Kalorimetrische Messungen der Verdampfungswärme des

Sauerstoffs bei normalem Druck sowie des Äthylens und Propylens unterhalb und oberhalb vom Atmosphärendruck. Z. Naturforsch., Abt. A, 4a: 117–124.

Deiters, U., 1981. A new semiempirical equation of state for fluids. I and II. Chem. Eng. Sci., 36: 1139–1159.

De Reuck, K.M. and Armstrong, R., 1979. A method of correlation using a search procedure, based on a step-wise least-squares technique, and its application to an equation of state for propylene. Cryogenics, 19: 505–512.

Ewers, J., 1981. Eine Methode zur Optimierung der Struktur von Zustandsgleichungen und ihre Anwendung zur Aufstellung einer Fundamentalgleichung für Sauerstoff. Dissertation Ruhr-Universität, Bochum.

Ewers, J. and Wagner, W., 1981. Eine Methode zur Optimierung der Struktur von Zustandsgleichungen und ihre Anwendung zur Aufstellung einer Fundamentalgleichung für Sauerstoff. VDI-Forschungsh., 609: 27–34.

Ewers, J. and Wagner, W., 1982. A method for optimizing the structure of equations of state and its application to an equation of state for oxygen. In: J.V. Sengers (Editor), Proc. Eighth Symp. on Thermophysical Properties. Am. Soc. Mech. Eng., Vol. 1: Thermophysical Properties of Fluids pp. 78–87.

Fletcher, R., 1971. A modified Marquardt subroutine for nonlinear least squares. United Kingdom Energy Authority Research Group Report AERE-R 6799, Harwell.

Frank, A. and Clusius, K., 1939. Präzisionsmessungen der Verdampfungswärme der Gase O_2, H_2S, PH_3, A, COS, CH_4 und CH_3D. Z. Phys. Chem. Abt. B, 42: 395–421.

Furukawa, G.T. and McCoskey, R.E., 1953. The condensation line of air and the heats of vaporization of oxygen and nitrogen. Nat. Advisory Comm. Aeronaut., Tech. Note 2969.

Goodwin, R.D. and Weber, L.A., 1969a. Specific heats of oxygen at coexistence. J. Res. Nat. Bur. Stand., 73 A: 1–12.

Goodwin, R.D. and Weber, L.A., 1969b. Specific heats of fluid oxygen from the triple point to 300 K at pressures to 350 atmospheres. J. Res. Nat. Bur. Stand., 73 A: 15–24.

Haar, L., Gallagher, J. and Kell, G.S., 1980. Thermodynamic properties for fluid water. In: J. Straub and K. Scheffler (Editors), Water and Steam—Their Properties and Current Industrial Applications. Proc. 9th ICPS, Pergamon Press, Oxford, pp. 69–82.

Hoge, H.J., 1950. Vapor pressure and fixed points of oxygen and heat capacity in the critical region. J. Res. Nat. Bur. Stand., 44: 321–345.

Jacobsen, R.T., 1972. The Thermodynamic Properties of Nitrogen from 65 to 2000 K with Pressures to 10000 Atmospheres, PhD. Thesis, Washington State University, Pullman.

McGarry, J., 1983. Correlation and prediction of the vapor pressures of pure liquids over large pressure ranges. Ind. Eng. Chem., Process Des. Dev., 22: 313–322.

Mochizuki, T., Sawada, S. and Takahashi, M., 1969. Reproducibility of the boiling point of oxygen and its pressure–temperature relation near 1 atmosphere. Jpn. J. Appl. Phys., 8: 488–495.

Pentermann, W., 1977. Experimentelle Bestimmung thermischer Zustandsgrössen von Sauerstoff. Dissertation Technische Universität Braunschweig.

Pentermann, W. and Wagner, W., 1978. New pressure–density–temperature measurements and new rational equations for the saturated liquid and vapour densities of oxygen. J. Chem. Thermodyn., 10: 1161–1172.

Pollak, R., 1974. Die thermodynamischen Eigenschaften von Wasser—dargestellt durch eine kanonische Zustandsgleichung für die fluiden homogenen und heterogenen Zustände bis 1200 Kelvin und 3000 bar. Dissertation Ruhr-Universität, Bochum.

Pool, R.A.H., Saville, G., Herrington, T.M., Shields, B.D.C. and Stavely, L.A.K., 1962. Some excess thermodynamic functions for the liquid systems argon + oxygen, argon + nitrogen, nitrogen + oxygen, nitrogen + carbon monoxide. Trans. Faraday Soc., 58: 1692–1704.

Schmidt, R., 1983. Eine neue Form einer Fundamentalgleichung und ihre Anwendung auf Sauerstoff. Dissertation Ruhr-Universität, Bochum.

Stewart, R.B. and Jacobsen, R.T., 1977. A thermodynamic property formulation for oxygen for temperatures from 55 K to 300 K and pressures to 34 MPa. In: A Cezairliyan (Editor), Proc. Seventh Symp. on Thermophysical Properties. Am. Soc. Mech. Eng. pp. 549–563.

Stewart, R.B., Jacobsen, R.T., Becker, J.H., Teng, J.C.J. and Mui, K.K.P., 1981. Thermodynamic properties of argon from the triple point to 1200 K with pressures to 1000 MPa. In: J.V. Sengers (Editor), Proc. Eighth Symp. on Thermophysical Properties. Am. Soc. Mech. Eng., Vol. 1: Thermophysical Properties of Fluids, pp. 97–113.

Straty, G.C. and Younglove, B.A., 1973. Velocity of sound in saturated and compressed fluid oxygen. J. Chem. Thermodyn., 5: 305–312.

Strobridge, T.R. 1962. The thermodynamic properties of nitrogen from 64 to 300 K between 0.1 and 200 atmospheres. Nat. Bur. Stand. Tech. Note 129.

Suyama, Y. and Oishi, J., 1976. Determination of vapor pressure–temperature relation of oxygen based on latent heat measurements of normal boiling point. Jpn. J. Appl. Phys., 15: 1037–1044.

Sytchev, V.V., Wasserman, A.A., Kozlov, A.D., Spiridonov, G.A. and Tsymarnyi, V.A., 1981. Thermodynamic properties of oxygen. Isdatelstwo standartov, Moscow (in Russian).

Tiggelman, J.L., 1973. Low temperature platinum thermometry and vapour pressures of neon and oxygen. Doctoral thesis, Univ. Leiden.

Van Dael, W., Van Itterbeek, A., Cops, A. and Thoen, J., 1966. Sound velocity measurements in liquid argon, oxygen and nitrogen. Physica, 32: 611–620.

Van Itterbeek, A. and Van Paemel, O., 1938. Measurements of the velocity of sound as a function of pressure in oxygen gas at liquid oxygen temperatures. Calculation of the second virial coefficient and the specific heats. Physica, 5: 593–604.

Van Itterbeek, A. and Zink, J., 1958. Measurements on the velocity of sound in oxygen gas under high pressure. Appl. Sci. Res., 7A: 375–385.

Wagner, W., 1970. Eine thermische Zustandsgleichung zur Berechnung der Phasengleichgewichte flüssig-gasförmig für Stickstoff. Dissertation Technische Universität Braunschweig.

Wagner, W., 1972. A method to establish equations of state exactly representing all saturated state variables—applied to nitrogen. Cryogenics, 12: 214–221.

Wagner, W., 1974. Eine mathematisch statistische methode zum aufstellen thermodynamischer gleichungen–gezeigt am beispiel der dampfdruckkurve reiner fluider stoffe. Fortschr.-Ber. VDI-Z. Reihe 3, Nr. 39.

Wagner, W., 1977. A new correlation method for thermodynamic data applied to the vapour pressure curve for argon, nitrogen and water. Report PC/T15, IUPAC Thermodynamic Table Project Centre, London.

Wagner, W., Ewers, J. and Pentermann, W., 1976. New vapour-pressure measurements and a new vapour pressure equation for oxygen. J. Chem. Thermodyn., 8: 1049–1060.

Wagner, W., Ewers, J., and Schmidt, R., 1982. An equation for the ideal-gas heat capacity of molecular oxygen for temperatures from 30 K to 3000 K. Ber. Bunsenges. Phys. Chem., 86: 538–540.

Wagner, W., Ewers, J., and Schmidt, R., 1984. An equation of state for oxygen vapour—second and third virial coefficients. Cryogenics, 24: 37–43.

Weber, L.A., 1970a. P–V–T, Thermodynamic and related properties of oxygen from the triple point to 300 K and pressures to 33 MN/m^2. J. Res. Nat. Bur. Stand. 74 A: 93–129.

Weber, L.A., 1970b. Density and compressibility of oxygen in the critical region. Phys. Rev. A, 2: 2379–2388.

Weber, L.A., 1977. Thermodynamic and Related Properties of Oxygen from the Triple Point to 300 K at Pressures to 1000 bar. NASA Reference Publication 1011, NBSIR 77–865.

Younglove, B.A. 1982. Thermophysical properties of fluids. I. Argon, ethylene, parahydrogene, nitrogene, nitrogen trifluoride, and oxygen. J. Phys. Chem. Ref. Data, 11, Supplement 1.